Comparison of Single- and Multi-date Landsat Data for Mapping Wildfire Scars in Ocala National Forest, Florida

Mary C. Henry

Abstract

Remote sensing techniques have been widely used to map fire scars in the western United States, but have not been thoroughly tested in the eastern portion of the country. In this study, a 1998 Landsat Thematic Mapper (TM) image and a 1999 Enhanced Thematic Mapper (ETM+) image were used to test different image enhancements and classification algorithms for mapping wildfire scars in Ocala National Forest, Florida. Single-date analysis was conducted using the 1999 image, while both images were used to complete multi-temporal analysis. Both single- and multi-date datasets were classified using a traditional method (maximum likelihood classification: MLC) and a non-parametric technique (classification and regression trees: CART). Comparison of all techniques showed that MLC of a single image (1999) resulted in high accuracy compared to the other methods and that principal components analysis (PCA) and multitemporal PCA provided the best spectral separability between burned and unburned areas.

Introduction

Florida is subjected to more lightning strikes than anywhere else in the U.S., with some areas experiencing more than 100 days each year with thunderstorms. Many of these lightning strikes result in wildfires, particularly during the dry, early part of the summer. Fire is an integral part of Florida's natural landscape and forest managers use prescribed fire as a management tool (Van Lear, 2000). Monitoring fires (both natural and prescribed) is an important goal for Florida's forest management staff in the USDA Forest Service, Florida Division of Forestry, and other agencies. Traditional burned area mapping techniques in these forests can be labor intensive and time-consuming, even when areas are relatively accessible by road. Automated burned area mapping could benefit forest managers and reduce the amount of fieldwork required to keep fire records current. Such an approach would also allow managers to reconstruct historical fire records where gaps in information exist. Remote sensing is a useful tool for burned area mapping, since it provides a synoptic view of the landscape that cannot be obtained through field visits and allows direct input of data into a geographic information system (GIS) database.

The majority of remote sensing-based fire research and burned area mapping in the U.S. has focused on states west of the Rocky Mountains (Cocke *et al.*, 2005; Holden *et al.*, 2005; Gong *et al.*, 2006), with a few exceptions (e.g., Maingi, 2005). The lack of research in the southeast may be attributable to factors such as more frequent cloud cover and generally easier accessibility in parts of the east, such as Florida. However, Florida's fire-prone vegetation communities hold many similarities to forest and shrub ecosystems of the southwestern U.S. and remote sensing may be a viable technique in these areas, as well. Results of this research could be applicable throughout pine forests and plantations of the southeastern United States.

This study investigates the use of satellite-based remotely sensed data for mapping burned areas in pine and scrub vegetation communities in Ocala National Forest, Florida. The following questions are addressed:

- Which techniques are best-suited to mapping burned areas in pine and scrub communities in Ocala National Forest?
- Which image enhancements best separate burned areas from unburned areas?
- Does a multi-temporal approach achieve higher accuracy than a single image?
- Does a non-parametric mapping approach achieve higher accuracy than traditional image classification techniques?

Background

As in many parts of the U.S., human-induced fire regime change (suppression and exclusion) has made a dramatic impact on Florida's pine forests. Prior to European settlement, many areas burned every two or three years, maintaining an extensive (37 million hectares) longleaf pine (*Pinus palustris*) forest over the southeastern coastal plain of the United States. These forests were home to hundreds of plant and animal species, many of which are now listed as endangered or threatened (Alavalapati *et al.*, 2002). It is currently estimated that only 4 percent of these forests remain, due to fire suppression, clearing for agriculture and human development, as well as plantation preference for other pine species (Alavalapati *et al.*, 2002).

Longleaf pine is a dominant species in Florida's high pine ecosystems, which have also been drastically reduced since European settlement (Christensen, 1991). One of the largest remaining stands of this type is located in Ocala National Forest (Myers, 1990). These sandhill communities

Department of Geography, Miami University, Oxford, OH 45056 (henrymc@muohio.edu).

Photogrammetric Engineering & Remote Sensing
Vol. 74, No. 7, July 2008, pp. 881–891.

0099-1112/08/7407–0881/$3.00/0

are located on sandy xeric "islands" within a matrix of scrub, another dwindling ecosystem in Florida. These scrub areas are dominated by evergreen shrubs such as oaks (*Quercus geminate, Q. myrtifolia*) and Florida rosemary (*Ceratiola ericoides*), with some scrub communities also having a pine overstory. Much of the largest area of Florida scrub (the Big Scrub complex) lies within Ocala National Forest.

Much research has been conducted in Florida's pine and scrub ecosystems (Brockway and Outcalt, 1998; Greenbery, 2003), but less work has been done at the landscape level (McCay, 2000). Some of this research has used GIS analysis and aerial photography to monitor historical landscape change in the Florida Panhandle (McCay, 2001) and central east coast (Duncan *et al.*, 1999).

Remote sensing has been used extensively for mapping fires in the western U.S. (Jakubauskus *et al.*, 1990; White *et al.*, 1996). Mapping of fires using remote sensing takes advantage of the distinct spectral reflectance properties of burned and unburned vegetation. Healthy, living vegetation reflects near-infrared energy and absorbs visible light (especially red wavelengths), while denuded areas (such as those subjected to a severe fire) typically reflect comparatively more energy across all of these wavelengths. These spectral differences allow clear delineation of recent fires using satellite-based remote sensing. Methods that exploit these characteristics are routinely used by the U.S. Forest Service to monitor and map the spatial extent of fires throughout the United States (for example, see **http://www.geomac.gov**), but managers at Ocala National Forest do not use these methods.

Burned Area Mapping in Conifer Forest

The rugged terrain in much of the forested area of western U.S. has necessitated the development of remote methods for mapping burned areas. Vast forested areas in the region are often inaccessible by road and located at high elevations and on steep slopes. One of the most widely used image enhancements for mapping wildfires in the western U.S. is the normalized burn ratio (NBR). This index was developed by Key and Benson (2003) as a variation of the normalized difference vegetation index (NDVI). Key and Benson (2003) replaced the red reflectance value with the mid-infrared reflectance value to make:

$$NBR_{TM} = (TM4 - TM7)/TM4 + TM7).$$

Bare soil reflects mid-infrared energy, so NBR emphasizes that contrast between bare and vegetated areas. This index has been adopted by the U.S. Forest Service for its Burned Area Emergency Response (BAER) teams. Researchers seeking to map burned areas in forested environments have also added this image enhancement to the suite of techniques being tested (Cocke *et al.*, 2005; Roy *et al.*, 2006). Miller and Yool (2002) tested NBR and other image enhancements to map the Cerro Grande Fire in New Mexico. Holden *et al.* (2005) used NBR and a thermally enhanced version of NBR ($NBRT_1$) to map burned areas in the Gila National Forest, New Mexico. In northern California, Pu and Gong (2004) tested NBR and NDVI in logistic regression and neural networks, and concluded that NBR and NDVI performed better than the original Landsat TM bands. In a study to map burn severity in the northern Rocky Mountains, Brewer *et al.* (2005) concluded that NBR was a widely applicable image enhancement that achieved good accuracy. While this image enhancement has met with success in the western states, it has not been widely tested in the ecosystems of the eastern U.S. One implicit objective of this study was to determine if techniques and enhancements used in western forests are also useful for similar applications in Florida.

Burned Area Mapping in Shrubland

Mediterranean shrublands, such as chaparral and coastal sage scrub communities of southern California, are adapted to stand-replacing fire regimes. The length of time between fires varies by dominant species and plant reproductive strategies. In many areas, fuels have accumulated for longer periods than had occurred historically and the results are often disastrous (e.g., San Diego County, 2003). Studies to map burned areas in Mediterranean regions have relied on the spectral contrast between healthy and dead, or removed vegetation (Diaz-Delgado *et al.*, 2004; Garcia and Chuvieco, 2004). The variety of techniques that have been successfully used to map burned areas in Mediterranean ecosystems include spectral vegetation indices such as NDVI (Diaz-Delgado and Pons, 2001; Gong *et al.*, 2001; Vafeides and Drake, 2005) and NBR (Brewer *et al.*, 2005). Rogan and Franklin (2001) and Riaño *et al.* (2002) used spectral mixture analysis to map burned areas in southern California chaparral. Another non-traditional method was developed by Koutsias *et al.* (2000) to map burned areas in the Mediterranean basin. Their method involved transforming false color composite images into their intensity-hue-saturation components. In a savanna ecosystem of South Africa, Hudak and Brockett (2004) used supervised classification of principal components analysis (PCA) to map burned areas. In this study, they also used multitemporal PCA to identify subtle burn areas when vegetation regrowth obscured burn evidence (Hudak and Brockett, 2004).

Multi-temporal Approaches to Burned Area Mapping

In addition to using single post-fire images to map burned areas, some researchers have included pre-fire images and used change detection methods (Miller and Yool, 2002). Fisher *et al.* (2003) used image differencing and PCA to map burned areas in Western Australia, while Rogan and Yool (2001) and Brewer *et al.* (2005) used a multitemporal PCA approach. The latter approach involves analyzing the principal components from a single multi-date image (all bands from both dates together in one file). Higher order components are expected to indicate changes between the two dates. Rogan and Yool (2001) also tested a multitemporal version of the Kauth-Thomas Transform (MKT) as developed by Collins and Woodcock (1996). The MKT is a linear image transformation that generates stable brightness, greenness, and wetness components from two images, in addition to change components for brightness, greenness, and wetness (Collins and Woodcock, 1996). When mapping burned areas in the Chihuahuan Desert of southeastern Arizona, Rogan and Yool (2001) obtained their highest classification accuracies using MKT change components. Multi-temporal approaches to mapping burned areas may be particularly advantageous in regions where there are land-cover types spectrally similar to burned areas (i.e., clear cuts).

Burned Area Mapping in Florida

Florida's ecosystems contain different plant species than forests of the western U.S. and Mediterranean shrublands, but they have distinct similarities in fire regime. Ponderosa pine forests (western U.S.) were historically maintained through frequent, low-intensity surface fires ignited by lightning during the late summer rainy season. The frequent fire kept stands open and clear of surface litter. This regime of frequent fire is common to the sandhill pine and flatwoods areas of Florida, including those dominated by longleaf pine (*Pinus palustris*), slash pine (*P. elliottii*), and pond pine (*P. serotina*). In contrast, chaparral of southern California is adapted to relatively infrequent, high-intensity, stand-replacing fires. This regime of burning all surface

vegetation is shared by Florida scrub species such as Florida rosemary (*Ceratiola ericoides*), scrub oaks (*Quercus geminata, Q. myrtifolia*), and even sand pine (*P. clausa*) (McConnell and Menges, 2002). The coexistence of these ecosystems with their distinctive fire regimes presented a unique opportunity to apply remote sensing techniques developed elsewhere in a new location. In Florida's pine and scrub ecosystems, as in other environments where burned areas are characterized by a significant reduction in green vegetation, it is reasonable to expect NBR to be able to differentiate burned and unburned areas.

There has been no work published on mapping burned areas in Florida's national forests using remote sensing. Current techniques for mapping fires include manual delineation on aerial photos and walking perimeters of larger fires with a hand-held GPS unit (Mark Clere, Ocala National Forest, personal communication). Smaller fires (<10 acres, or 4.04 ha) are only mapped as points, and therefore their spatial extents are not delineated. Wildfires in Ocala National Forest are currently recorded in paper reports that include details of ignition date and time, point location, and estimated fire size.

Rule-based Image Classification

Traditional image classification techniques assume that data follow a Gaussian distribution and can only be used on continuous data. Rule-based methods, such as classification and regression trees (CART), do not rely on these assumptions and can include ordinal and nominal datasets. This flexibility allows continuous data such as spectral bands, vegetation indices, and topographic variables to be used in conjunction with categorical data, such as land-cover and some forest stand data. CART techniques do not require expert knowledge of a study area, but only delineation of training sites, as in traditional supervised classification methods. Once training sites have been selected to represent each land-cover class, a computer algorithm generates rules based on input datasets. Some CART programs are capable of *winnowing* attributes, or excluding input datasets that do not contribute to the rules. This additional information can be particularly helpful to the user in determining which data are most critical in mapping the desired land-cover classes. Application of CART and other rule-based methods include studies to map vegetation types in the National Parks system (Brown de Coulston *et al.*, 2003), Norway (Vikhamar and Fjone, 2004), Kaibab National Forest, Arizona (Joy *et al.*, 2003), the Greater Yellowstone Ecosystem (Lawrence and Wright, 2001), and globally (DeFries and Chan, 2000). Other studies tested CART for mapping land-use in Beijing, China (Li *et al.*, 2000), vegetation patterns in North Carolina (Taverna *et al.*, 2005), and impervious surfaces in South Carolina (Hodgson *et al.*, 2003). Rogan *et al.* (2003) used CART methods to monitor vegetation changes in San Diego County, California. Pal and Mather (2003) investigated the effects of training sample size and data dimensionality on CART techniques and found that for both parameters, accuracy increased with increasing training samples and data inputs, but reached a threshold where additional training samples or input bands did not improve accuracy. Studies making direct comparisons between CART classifiers and traditional methods, such as maximum likelihood classifiers, or MLC (Freidl and Brodley, 1997) have met with mixed results, depending on land-cover classes tested and level of detail (Joy *et al.*, 2003). Brewer *et al.* (2005) compared multi-temporal mapping methods, including CART to map burned areas in southern Montana. It is clear that more research is needed to determine when CART methods are appropriate for burned area mapping applications.

Methods

The goal of this study was to compare burned area mapping methods in Ocala National Forest. Four techniques were compared: maximum likelihood classification (MLC), classification and regression trees (CART) for both single-date and multi-date analysis. Wildfires from 1998 and 1999 (up to 23 October 1999) were mapped using these methods. This approach was taken to determine which classifier is best suited to the task, whether single- or multi-date analysis was more effective, and assess which image enhancements most successfully separate burned and unburned vegetation. Only supervised classification techniques were tested, due to the specificity of the burned areas and the small proportion of the landscape that they represent. The 1998 fire season was chosen due to its historical significance, as one of the worst fire seasons on record in Florida. A 1999 image was selected as the subsequent year for comparison.

Study Area

Ocala National Forest is located in central Florida, approximately 55 km north-northwest of Orlando (see Figure 1). The forest contains a range of plant communities such as pine flatwoods, sandhill pine, and pine scrub. The spatial distribution of sandhill pine and sand pine scrub is highly dependent on fire regime. If fires are frequent and low-intensity, sandhill pine will dominate with stands of longleaf pine. If fires are infrequent and high-intensity, the sand pine scrub will be favored. Ocala National Forest is highly managed and heavily used for recreation purposes, with roads, campgrounds, and picnic areas found throughout the forest. A naval bombing range is also located in the southern district (Seminole District). The Forest Service maintains an active prescribed burning program with some areas of the Forest on two- or three-year burn rotation (longleaf pine).

One of the worst fire seasons on record in Florida was 1998, with over 120,000 ha burned (79.2 percent of which were lightning ignited). However, Ocala National Forest did not experience an unusually severe fire season that year. The aggressive prescribed burning program likely contributed to the lack of extreme fires. The vegetation communities played a role as well, since mesic sites tended to be hardest hit that year (Breininger *et al.*, 2002).

Figure 1. Location of Ocala National Forest, Florida.

Data

Landsat Data

One Landsat Thematic Mapper (TM) image and one Enhanced Thematic Mapper Plus (ETM+) image were obtained for analysis. The TM image was acquired 31 December 1998 (scene ID: L5016040009836510) and the ETM+ image was acquired 23 October 1999 (scene ID: L7016040009929650). Low sun angle images were acquired, because they correspond to the short dry season in Central Florida. By selecting these images, it was possible to avoid the cloud cover present in the region during most of the year. Central Florida's gently rolling topography does not produce visible topographic shadows, so sun angle is not as critical as in areas with rugged terrain. The 1999 image was selected because it was earlier in the year (closer to the end of the fire season), but no matching cloud-free image was available for 1998. Landsat-5 DNs (1998 image) were transformed to Landsat-7 equivalent DN values prior to pre-processing and analysis (USGS, 2001). Both images were converted to reflectance using the COST model (Chavez, 1996), which reduces image haze effects.

Wildfire Data

Ocala National Forest maintains detailed records of wildfires occurring within the Forest. These documents include: fire name, location (description, township and range, latitude and longitude), point of ignition, time of ignition, time of discovery, and estimated fire size). The reports are quite detailed, but are in paper form only and do not include maps (paper or digital). There are also time periods with missing or incomplete data. These fire records were used to identify recently burned areas for selecting training and test sites. Since the extent of each fire was not spatially explicit, only fires visible on one or both of the images were used as training sites. Reports for 1998 and 1999 are considered fairly complete (Tammy Milton, USDA Forest Service, personal communication).

USFS GIS Data

Ocala National Forest supplied GIS data including roads, forest boundary, forest stand data, prescribed burn data, and elevation data (USGS 30-meter DEM). These data assisted in location of training and test sites and verified the geospatial accuracy of the image data (i.e., road locations matched images, etc.)

Analysis Procedures

Methods varied by which mapping technique was tested. In this section, these procedures are described in detail. To clarify the image processing steps, a flow chart outlining these procedures is shown in Figure 2.

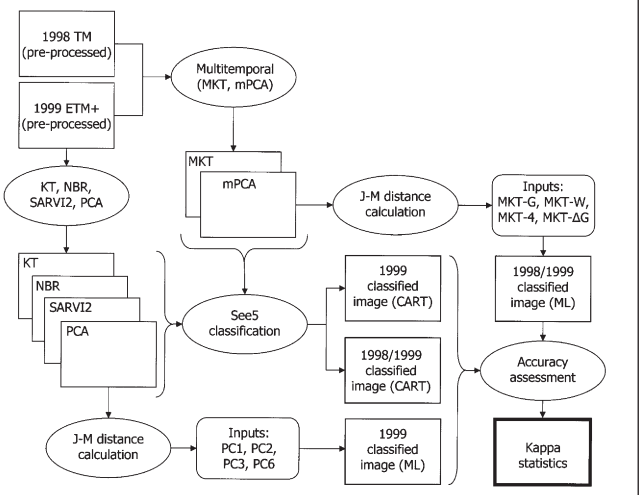

Figure 2. Flowchart of image processing procedures.

Training Site Selection

Training sites were selected for six land-cover classes: water, 1998 fire, 1999 fire, forest, bare/developed, and riparian vegetation (see Table 1). Although it was not necessary to distinguish all of these classes in the mapping procedure, they were kept separate for training purposes due to spectral disparities between them (e.g., water versus forest). It was also important to distinguish fires from other bare areas, so clear cuts were included in the training procedure. Some classes (water, forest, riparian vegetation) were easily located using Landsat TM and ETM+ false color composites, while others were identified using USFS GIS data (e.g., stand data). Riparian vegetation was listed as a separate class, since it had a distinctive appearance in the 1998 TM image (due to phenological differences). Locations of wildfires occurring in 1998 and 1999 were determined from U.S. Forest Service reports (see Wildfire Data above). Only fires that were visibly distinct were used as training sites. Point fire locations with no visible fire scar were excluded. Training sites were delineated on-screen using the data sources listed above, to select a total of 5,606 training pixels.

Image Enhancements

A range of image enhancements were used in this study to assess the separability of land-cover classes. Single-date analysis included the Tasseled Cap Transform (KT), Soil Adjusted Atmospherically Resistant Vegetation Index (SARVI2), which is a variation of the Normalized Difference Vegetation

TABLE 1. CLASSES USED IN THE MAPPING PROCEDURES. PRIOR PROBABILITIES WERE USED IN MAXIMUM LIKELIHOOD CLASSIFICATIONS

Class name	Abbreviation	Description	# Training pixels	Prior probabilities
Water	Water	Lakes, open water	858	0.10
1998 fire	98fire	Fires occurring between 1/1/1998 and 12/31/1998	978	0.01
1999 fire	99fire	Fires occurring between 1/1/1999 and 10/23/1999	1060	0.01
Forest	Forest	Vegetated areas including forest, woodland, and shrubland	1104	0.73
Bare/developed	Bare	Recent clear cuts, developed areas, roads, exposed soil	1257	0.05
Riparian vegetation	Rveg	Riparian forest, aquatic vegetation	349	0.10

Index (NDVI), Normalized Burn Ratio (NBR), and Principal Components Analysis (PCA). The KT Transform applies coefficients to the Landsat ETM+ data to create three new components: Brightness, Greenness, and Wetness. Each of these components emphasizes a different aspect of the original image data. The Brightness image shows bare soil and rock as bright, but water and vegetation are dark. Greenness shows vegetated areas as bright and bare areas dark. KT-Wetness corresponds to moisture content in vegetation, so that healthy green vegetation appears bright, but dead vegetation appears dark. Patterson and Yool (1998) successfully mapped fire severity in the southwest using the KT Transform.

The NDVI is calculated as a ratio that accentuates the differences between red and near-infrared reflectance. Areas with high amounts of healthy green vegetation appear bright in an NDVI image. Studies in many different environments have found relationships between NDVI and canopy cover (Larsson, 1993), sunlit canopy fraction (Hall *et al.*, 1995) and primary production (Tucker and Sellers, 1986). NDVI has also been used extensively to evaluate fire-related forest conditions (Marchetti *et al.*, 1995; White *et al.*, 1996). Several variations of NDVI have been developed to minimize effects of soil background and atmospheric attenuation, such as the soil-adjusted vegetation index (SAVI) and the soil-adjusted atmospherically resistant vegetation index (SARVI2) (Huete *et al.*, 1997). The normalized burn ratio (NBR) is a variation of NDVI developed specifically for burned area mapping (Key and Benson, 2003).

Principal Components Analysis (PCA) is a method that can be used to reduce dimensionality in a multivariate dataset. Analyzing image data with this technique results in image enhancements, as well as information on loadings for each band (eigenvectors and eigen-matrices). These loadings are informative in that they reveal which original inputs are most strongly represented in the transformed data. While direct interpretation of PCA images can be difficult (i.e., which component represents which land-cover type), researchers have found the resulting images to be useful in distinguishing land-cover (Liu *et al.*, 2003) and forest types (Maingi and Luhn, 2005).

Multi-date enhancements consisted of a multi-temporal PCA (MPCA) and multi-temporal KT (MKT). The multi-temporal version of PCA has similar advantages to those described above, but inputs consist of data from more than one image date. Lower order components typically represent stable aspects of the landscape, while changes appear in the higher order components. The MKT was developed by Collins and Woodcock (1996) and results in stable Brightness, Greenness, Wetness components for the two dates, plus change components for each (ΔB, ΔG, ΔW). Collins and Woodcock (1996) compared MKT to other change detection techniques and found it was more sensitive to changes in forest conditions (tree mortality) and less affected by atmospheric differences than other image transformations. For this study, the three stable components (bands 1, 2, 3 from the output) and the three change components (bands 7, 8, 9) in separability tests were used.

Classification Approaches

Single-date analysis used only the 1999 image to detect fires from both 1998 and 1999. This allowed class consistency between both single- and multi-date mapping procedures, enabling direct comparison of the techniques (i.e., 1999 fires that could not be mapped from 1998 data). Following preprocessing, the 1999 ETM+ image was used to calculate KT, NBR, SARVI2, and PCA. Jeffries-Matusita (JM) distances were used to analyze separability of the six land-cover classes for three groups of data: ETM+ bands (ETM1, ETM2, ETM3, ETM4, ETM5, ETM7), spectral vegetation indices, or SVIs (KT-brightness, KT-greenness, KT-wetness, NBR, SARVI2), and PCA (PC1, PC2, PC3, PC4, PC5, PC6). The best four-band combination consisted of PC1, PC2, PC3, and PC6 (best minimum separability was 1086.03.) These inputs were used in a maximum likelihood classification (see below).

Two multitemporal enhancements were applied to the 1998 TM image and 1999 ETM+ image: MKT and MPCA. JM distances were calculated for each set of data and the best four-band combination used in a maximum likelihood classification (see below). The best four-band combination consisted of MKT-G, MKT-W, MKT-4, and MKT-ΔG (best minimum separability was 1396.27.)

Using training sites and band combinations discussed above, MLC was run on both the 1999 ETM+ image (PC1, PC2, PC3, PC6) and the multitemporal data set (MKT-G, MKT-W, MKT-4, and MKT-ΔG). Prior probabilities, based on visual estimates of each cover type's proportion of the landscape, were used in both classifications (see Table 1). Fires covered a very small portion of the landscape, so low probabilities were assigned to those classes (1998 fires and 1999 fires) to avoid over-classifying them. All non-fire classes were condensed into a "no fire" class, so that final classes were no fire, 1998 fire, and 1999 fire. Accuracy assessment was run on both resulting maps (single- and multi-date) and is discussed below.

For the CART mapping procedures, training sites were used to generate a raster format training layer consisting of class locations. CART analysis was run on the 1999 ETM+ data using all original bands and generated enhancements (Table 2), allowing the See5 (C 5.0) program to winnow out unnecessary layers. The same procedure was run on the complete multi-date data set (see Table 2 for inputs). All non-fire classes were condensed into a "no fire" class following classification to simplify interpretation of the results. Accuracy assessment was conducted on both CART maps and is discussed below.

Comparison of Maps

In order to make quantitative comparisons between the four maps (multi-date versus single-date, CART versus MLC), each map's accuracy was assessed using approximately 300 stratified random test points. To avoid bias, no test points were selected within the training sites. Reference classes were determined using field observations and visual interpretation of the TM and ETM+ images. For each map, several accuracy measures were calculated. All maps had overall accuracy (percentage), overall Kappa, producer's and user's accuracy for each class, and class Kappa. CART maps also had internal accuracy calculated from the training and test data. All measures were used to compare maps and determine the best method for mapping burned areas. Additionally, qualitative comparisons were made through visual inspection of final maps. Because burned areas account for such a small portion of the landscape, this assessment was included to provide a complete picture of the results.

Results and Discussion

The goal of this study was to determine which techniques are best-suited to mapping burned areas in pine and scrub communities in Ocala National Forest, Florida. Below, each specific question from the Introduction is restated and results summarized.

Image Enhancements Which Best Separate Burned Areas from Unburned Areas *MLC Mapping*

JM distances were used to select inputs to the MLC for both single-date and multi-temporal analysis. For single-date analysis, data were divided into three datasets: ETM+ bands

TABLE 2. INPUTS TO CART CLASSIFICATION FOR (A) 1999 IMAGE DATA, AND (B) MULTI-TEMPORAL DATA. NUMBERS INDICATE THE NUMBER OF RULES USING THAT INPUT

	Number of Rules						
Input	Water	98fire	99fire	Forest	Bare	Rveg	*Total*
ETM 1		1	1			1	*3*
ETM 2		1		1		1	*3*
ETM 3							
ETM 4	1	3	2	4	1	2	*13*
ETM 5							
ETM 7	1	3	3	4		2	*13*
KT-B		4	1	1		1	*7*
KT-G							
KT-W				1			*1*
KT-4		1		2		1	*4*
KT-5							
KT-6				1			*1*
NBR							
SARVI2		1		1			*2*
PC1		1		1		1	*3*
PC2							
PC3				1		2	*3*
PC4							
PC5							
PC6							

(a)

	Number of Rules						
Input	Water	98fire	99fire	Forest	Bare	Rveg	*Total*
MKT-B		4	1	2	3		*10*
MKT-G		1	1	1	1	1	*5*
MKT-W							
ΔKT-B		2			4		*6*
ΔKT-G		2		1	2	1	*6*
ΔKT-W		3	1	1	2	2	*9*
MPC1	1		1				*2*
MPC2							
MPC3		1		1	3	2	*7*
MPC4							
MPC5		4	1	1	6	1	*13*
MPC6							
MPC7							
MPC8							
MPC9							
MPC10							
MPC11							
MPC12							

(b)

(1, 2, 3, 4, 5, and 7), spectral vegetation indices (KT-B, KT-G, KT-W, NBR, SARVI2), and PCA (PC1, PC2, PC3, PC4, PC5, PC6). The best four-band combinations from each dataset are shown in Table 3. The dataset with the best minimum separability was PCA; PC1, PC2, PC3, and PC6 were selected based on best minimum separability (JM distance = 1086.03). This band combination provided slightly better separability than using the ETM+ reflectance bands or spectral vegetation indices (see Table 3). It was difficult to separate riparian vegetation from forest using the 1999 image, since the riparian vegetation was photosynthetically active at image acquisition. In the 1998 TM scene, these

TABLE 3. SEPARABILITY FOR EACH DATA SET. NUMBERS SHOWN ARE JEFFRIES-MATUSITA DISTANCES FOR EACH PAIR OF CLASSES. ONLY THE BEST FOUR-BAND COMBINATIONS FOR EACH DATA SET ARE SHOWN

ETM+ Bands: 2 4 5 7 — Min. 1068

	Forest	Bare	Water	Rveg	99fire	98fire
Forest	0	1376	1414	1068	1412	1400
Bare		0	1414	1401	1411	1298
Water			0	1414	1414	1414
Rveg				0	1414	1405
99fire					0	1312
98fire						0

SVIS: B G W SARVI2 — Min. 1061

	Forest	Bare	Water	Rveg	99fire	98fire
Forest	0	1400	1414	1061	1412	1410
Bare		0	1414	1412	1413	1280
Water			0	1414	1414	1414
Rveg				0	1414	1413
99fire					0	1336
98fire						0

MKT: G W 4 ΔG — Min. 1396

	Forest	Bare	Water	Rveg	99fire	98fire
Forest	0	1405	1414	1402	1414	1402
Bare		0	1414	1414	1410	1400
Water			0	1414	1414	1414
Rveg				0	1414	1396
99fire					0	1414
98fire						0

PCA: PC1 PC2 PC3 PC6 — Min. 1086

	Forest	Bare	Water	Rveg	99fire	98fire
Forest	0	1378	1414	1086	1412	1400
Bare		0	1414	1403	1411	1287
Water			0	1414	1414	1414
Rveg				0	1414	1406
99fire					0	1313
98fire						0

MPCA: PC1 PC2 PC4 PC5 — Min. 1382

	Forest	Bare	Water	Rveg	99fire	98fire
Forest	0	1402	1414	1382	1414	1408
Bare		0	1414	1414	1413	1393
Water			0	1414	1414	1414
Rveg				0	1414	1409
99fire					0	1414
98fire						0

areas were visually distinct due to phenological changes (riparian vegetation was senescent). Bare areas were spectrally similar to 1998 fires in the 1999 ETM+ image, but JM distances were close to 1300 for all three groups of data. The PCA bands were selected based on best minimum separability, but all groups of data provided similar separability for all classes. All classes were separable (JM distance near 1414), except for those cases discussed above.

The four-band combinations for each dataset were selected by their best minimum JM distances. In the case of the ETM+ data, ETM2, ETM4, ETM5, and ETM7 were the best combination. Exclusion of the blue band (ETM1) is common (it is highly correlated with green reflectance and more prone to atmospheric attenuation), but removal of the red band (ETM3) was unexpected. Red reflectance is often useful in vegetation studies, especially in combination with near infrared reflectance, since the "red edge" can be exploited. Healthy, green vegetation reflects near infrared radiation and absorbs red light, so the difference between the two is linked to vegetation health or amount. For the vegetation indices, reducing the dataset to four bands, meant excluding only one band (NBR). This was also an interesting result, since that index was designed specifically for mapping burned areas. However, this phase of the analysis included four non-fire classes, so it appears to be less advantageous to use NBR to map them. PCA bands included the first three components, which accounted for 99.3 percent of the total image variance, and the sixth PC which only accounted for 0.13 percent of the total image variance.

Multi-date analysis compared two datasets: MKT and MPCA. The four-band combinations for each dataset were selected based on best minimum JM distance (see Table 3). For multi-date MLC, MKT stable components for greenness, wetness, component 4, and the change in greenness component were selected. The MPCA four-band combination with best minimum separability was PC1, PC2, PC4, and PC5. PC1 and PC2 accounted for 98.46 percent of the multi-date image variance (94.01 percent and 4.45 percent, respectively). PC4 and PC5 account for 0.71 percent of the total variance (0.44 percent and 0.26 percent, respectively). The last five PCs (PC8 through PC12) accounted for less than 0.1 percent of the total image variance. Both MPCA and MKT indicated good separability for all classes (minimum JM distances for both were near 1400). Classes that were spectrally confused (or less separable) using the 1999 image were easily separable using the 1998 TM and 1999 ETM+ data together.

CART Mapping

For single-date mapping, C5 winnowed out nine of the original 20 inputs, including ETM3 (red), ETM5 (mid-infrared), KT-Greenness, and NBR (Table 2). Higher order PCs were also excluded from the analysis. The bands/enhancements that were used most often (appeared in the most CART rules) were ETM4 (near infrared) and ETM7 (mid-infrared). These bands are useful for assessing vegetation conditions and distinguishing bare ground from vegetation cover. It is interesting to note that these two bands are also the inputs to the NBR, which was excluded from the analysis. KT-Brightness was also used in several rules, including those for mapping 1998 fires and 1999 fires.

CART analysis of multi-temporal image enhancements used all MKT components, except one (Stable MKT-Wetness), and three of the first six principal components (Table 2). The enhancement used in the most rules was MPC5. In multi-temporal PCA, higher order components often represent change between the two input images. Areas burned in 1998 would have experienced some recovery between the two images and any new 1999 fires would also appear as a change. This may explain the apparent usefulness of MPC5. Stable MKT-Brightness was also used in several rules, including those for mapping 1998 fires and 1999 fires.

Accuracy of the Multi-temporal Approach versus the Single Image Approach

Accuracy was assessed in several ways for each classification. Both MLC and CART accuracy was evaluated using a traditional error matrix and the Kappa statistic. CART accuracy was also calculated using internal test data. Results of each accuracy assessment are shown in Table 4. For MLC, using the multi-temporal dataset improved accuracy slightly over the single-date (no change in overall accuracy; Kappa increased 0.769 to 0.775), but for CART, accuracy decreased slightly with the multi-temporal dataset (89.86 percent to 89.19 percent and 0.736 to 0.725). However, internal accuracy was slightly better (0.7 percent, 2.5 percent error rate, rather than 2.9 percent and 6.3 percent) using the multi-temporal data.

At the class level, 1999 fires were mapped more accurately than 1998 fires (Table 5) for all maps. Single- and

TABLE 4. SUMMARY OF CLASSIFICATION ACCURACIES FOR EACH TECHNIQUE

	Accuracy		Error Rates	
	Overall	Kappa	Training	Test
MLC/single-date	91.22%	0.769	–	–
MLC/multi-date	91.22%	0.775	–	–
CART/single-date	89.86%	0.736	2.90%	6.30%
CART/multi-date	89.19%	0.725	0.70%	2.50%
Max – min	*2.03%*	*0.050*		

TABLE 5. SUMMARY OF ACCURACY ASSESSMENT BY CLASS

MLC 1999	**Reference data**					
	No fire	1999 fire	1998 fire	Prod acc	Users acc	Kappa
No fire	215	1	14	95.13%	93.48%	0.724
1999 fire	3	27	0	96.43%	90.00%	0.890
1998 fire	8	0	28	66.67%	77.78%	0.771
MLC Multi	**Reference data**					
	No fire	1999 fire	1998 fire	Prod acc	Users acc	Kappa
No fire	214	0	11	94.69%	95.11%	0.793
1999 fire	1	27	2	96.43%	90.00%	0.890
1998 fire	11	1	29	69.05%	70.73%	0.659
CART 1999	**Reference data**					
	No fire	1999 fire	1998 fire	Prod acc	Users acc	Kappa
No fire	213	3	12	94.25%	93.42%	0.722
1999 fire	3	23	0	82.14%	88.46%	0.873
1998 fire	10	2	30	71.43%	71.43%	0.667
CART Multi	**Reference data**					
	No fire	1999 fire	1998 fire	Prod acc	Users acc	Kappa
No fire	211	1	12	93.36%	94.20%	0.755
1999 fire	2	27	4	96.43%	81.82%	0.799
1998 fire	13	0	26	61.90%	66.67%	0.612

multi-date MLC maps had the same accuracy for 1999 fires, with the single-date MLC slightly higher for 1998 fires (based on user's accuracy and Kappa). The single-date CART map had higher user's accuracy and Kappa than the multi-date CART map for both 1998 and 1999 fires.

Visual inspection of the maps (Figure 3) shows that all methods over-classified fires, particularly 1998 fires. Of the four known fire locations indicated on the map, two were clearly identified (one from 1998, one from 1999). Two others were not mapped as fires and may have been very small or of low intensity. Either situation could allow sufficient vegetation growth that would obscure the burned area. Grass-dominated areas such as longleaf pine/wire grass "islands" were often mistakenly mapped as fires due to senescent grasses being spectrally confused with burned areas. When prescribed burns were removed from the maps, many "non-fires" disappeared (Figure 4). Prescribed burns were not included as training sites in this study, since fire intensity and consequent landscape characteristics are quite disparate for wildfires and prescribed burns. The map most changed by removal of prescribe burns appears to be the MLC multi-temporal map, while the multi-temporal CART map still showed several incorrectly mapped 1999 fires.

Accuracy of a Non-parametric Mapping Approach versus a Traditional Image Classification Technique

For both multi- and single-date analysis, MLC had slightly higher accuracy than CART, but the differences are not large (2.03 percent between best and worst overall accuracy; 0.05 between best and worst Kappa). CART was more likely to over-classify fires than MLC (see Figure 3). Because the MLC included prior probabilities (Table 1), the area mapped as fire in those classifications was much lower.

At the class level, MLC had slightly higher Kappa values for both 1998 fires and 1999 fires (Table 5). There was a greater difference between multi-temporal CART and multi-temporal MLC: almost 10 percent higher accuracy for MLC mapping of 1999 fires, with a smaller difference between them for 1998 fires. MLC also had higher user's accuracies for both single-date and multi-temporal classification. Visual comparison of the maps indicates that fires were over-classified by all techniques, but both CART maps classified more areas as fires than the MLC (Figure 3).

Conclusions and Recommendations

As would be expected, recent fires were more accurately mapped than older fires. Vegetation recovery following fire

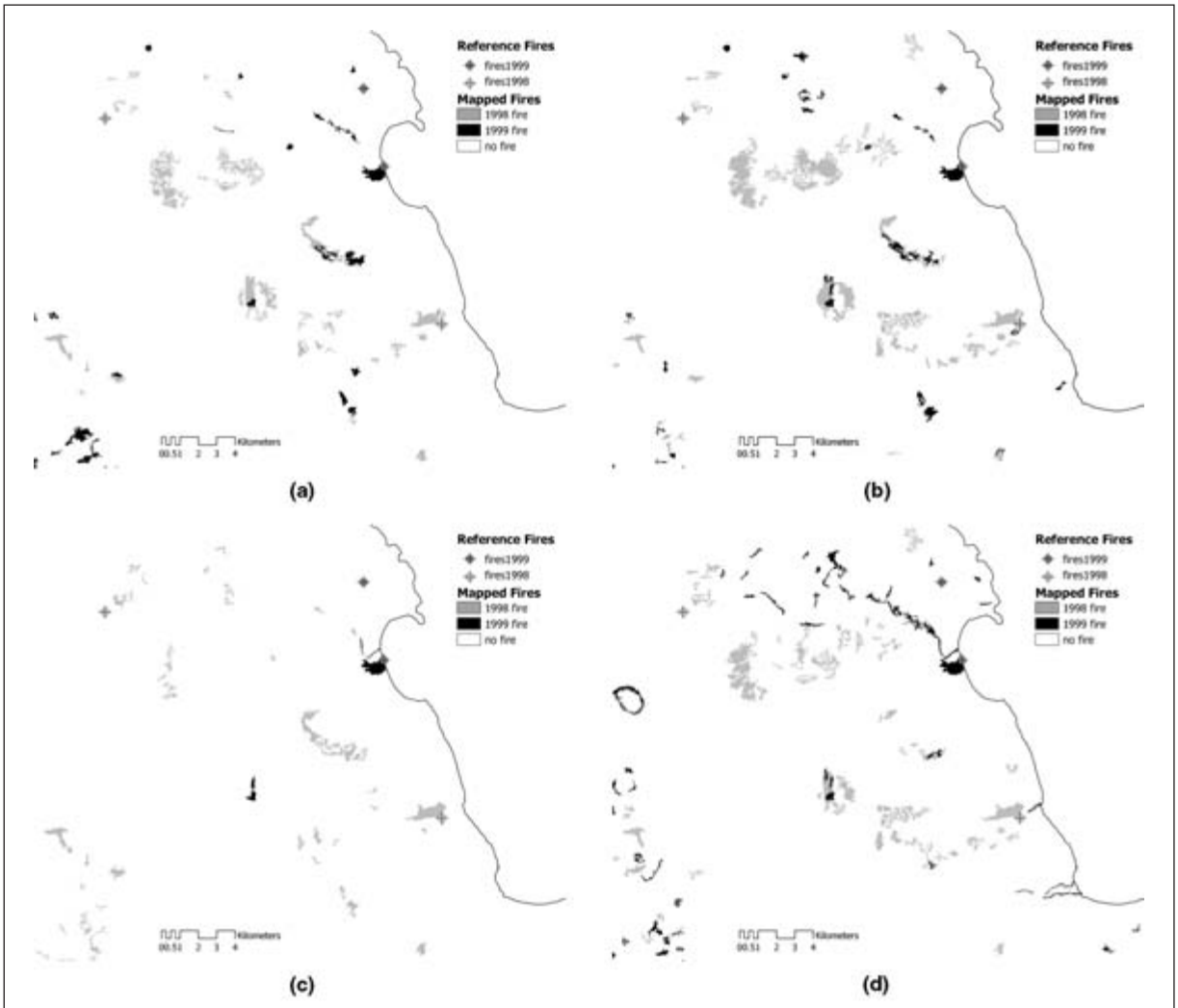

Figure 3. Spatial subset of resulting wildfire scar maps: (a) single-date MLC, (b) single-date CART, (c) multi-temporal MLC, and (d) multi-temporal CART.

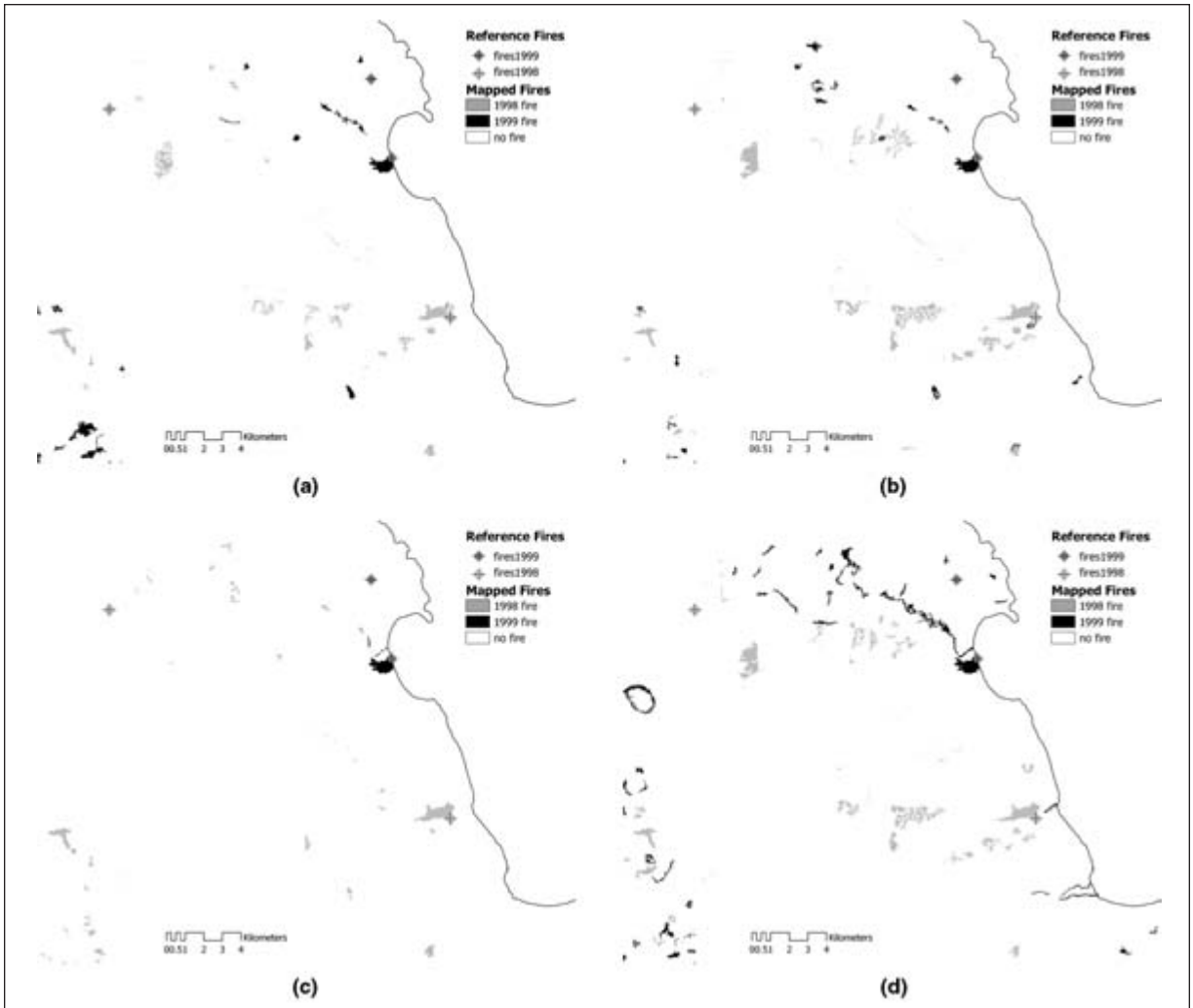

Figure 4. Portion of resulting wildfire scar maps with prescribed burns from 1998 and 1999 removed: (a) single-date MLC, (b) single-date CART, (c) multi-temporal MLC, and (d) multi-temporal CART.

is especially rapid in Florida due to warm temperatures and high moisture levels throughout the year. As a result, only high severity burned areas persist on the landscape. This was especially evident in the class accuracies, where the best mapping technique only obtained a Kappa of 0.771 for 1998 fires (77.78 percent user's accuracy). The highest accuracies for 1999 fires (Kappa = 0.890, user's accuracy = 90 percent) were obtained using MLC. In this case, single- and multi-date MLC had identical accuracies for 1999 fires. One could argue that the multi-temporal MLC was slightly better, since most of the confusion for 1999 fires occurred with 1998 fires, rather than "no fire." These results show that using a more complex algorithm does not always translate to higher accuracy. For many applications CART and multi-temporal analysis are superior (e.g., mapping forest types with subtle spectral differences), but researchers should choose their methods carefully.

Image enhancements that have been used in one region are not necessarily transferable to other regions. NBR has been widely used to map burned areas in the western U.S., but for this application was not found to be as useful as other enhancements. Rapid vegetation recovery in this humid subtropical climate may have contributed to this trend, since NBR uses bare soil as an indicator of burned areas.

Accuracy differences between single- and multi-date techniques were mostly small, although accuracies for single-date mapping were slightly higher. These findings suggest that using single-date imagery to inventory fires for a particular year would be the best course of action. Using one image (rather than multi-temporal analysis) eliminates the problem of relative or absolute radiometric correction between dates, spatial registration errors, frequent cloud cover, and phenological differences. MLC performed better than CART in almost every comparison, from overall accuracy to class-level Kappa. MLC is also an algorithm that is simple to perform in most image processing software packages, whereas CART is not as widely available. For the landscape studied in this research, wildfires only represent a small fraction of the landscape. Using MLC with prior probabilities has the flexibility to allow users to define this variable. While accuracy levels are high, it is clear from visual inspection that some fires were missed and other areas were incorrectly mapped as fires, even in the maps with the highest accuracy. Future work could compare maps in quantitative ways other than accuracy measures.

Other future research could test similar procedures with different image dates and different seasons (if cloud-free images are available). It would also be helpful in the future to collect burn severity data in order to assess how long particular burned areas persist on the landscape and how long they can be detected from satellite sensors. Additional data on weather conditions and other factors controlling regeneration could also provide insight into the limitations of mapping burned areas in this environment. Finally, other novel approaches to land-cover mapping could be tested, such as spectral mixture analysis and object-oriented classification.

Acknowledgments

This research was supported in part by a Committee for Faculty Research Grant from Miami University. The author wishes to thank Ocala National Forest personnel for their cooperation and field visit assistance from Andy Bernard, Jim Thorsen, Kathy Bronson, and Mark Clere. Wildfire data were provided by Tammy Milton, Ocala National Forest. The author also appreciates editorial comments from Dr. John Maingi and the three anonymous reviewers.

References

Alavalapati, J.R.R., G.A. Stainback, and D.R. Carter, 2002. Restoration of the longleaf pine ecosystem in private lands in the US South: An ecological economic analysis, *Ecological Economics*, 40:411–419.

Breininger, D.R., B.W. Duncan, and N.J. Dominy, 2002. Relationships between fire frequency and vegetation type in pine flatwoods of East-Central Florida, USA, *Natural Areas Journal*, 22(3):186–193.

Brewer, C.K., J.C. Winne, R.L. Redmond, D.W. Opitz, and M.V. Mangrich, 2005. Classifying and mapping wildfire severity: A comparison of methods, *Photogrammetric Engineering & Remote Sensing*, 71(11):1311–1320.

Brockway, D.G., and K.W. Outcalt, 1998. Gap-phase regeneration in longleaf pine wiregrass ecosystems, *Forest Ecology and Management*, 106:125–139.

Brown de Colstoun, E.C., M.H. Story, C. Thompson, K. Commisso, T.G. Smith, and J.R. Irons, 2003. National Park vegetation mapping using multitemporal Landsat 7 data and a decision tree classifier, *Remote Sensing of Environment*, 85:316–327.

Chavez, P.S., Jr., 1996. Image-based atmospheric corrections – Revisited and improved, *Photogrammetric Engineering & Remote Sensing*, 60:1285–1294.

Christensen, N.L., 1991. Vegetation of the southeastern coastal plain, *North American Terrestrial Vegetation* (M.G. Barbour and W.D. Billings, editors), Cambridge University Press, Cambridge.

Cocke, A.E., P.Z. Fulé, and J.E. Crouse, 2005. Comparison of burn severity assessments using Differenced Normalized Burn Ratio and ground data, *International Journal of Wildland Fire*, 14(2):189–198.

Collins, J.B., and C.E. Woodcock, 1996. An assessment of several linear change detection techniques for mapping forest mortality using multitemporal Landsat TM data, *Remote Sensing of Environment*, 56:66–77.

DeFries, R.S., and J.C. Chan, 2000. Multiple criteria for evaluation machine learning algorithms for land cover classification from satellite data, *Remote Sensing of Environment*, 74:503–515.

Diaz-Delgado, R., and X. Pons, 2001. Spatial patterns of forest fires in Catalonia (NE of Spain) along the period 1975–1995: Analysis of vegetation recovery after fire, *Forest Ecology and Management*, 147:67–74.

Diaz-Delgado, R., F. Lloret, and X. Pons, 2004. Spatial patterns of fire occurrence in Catalonia, NE, Spain, *Landscape Ecology*, 19(7):731–745.

Duncan, B.W., S. Boyle, D.R. Breininger, and P.A. Schmalzer, 1999. Coupling past management practice and historic landscape change on John F. Kennedy Space Center, Florida, *Landscape Ecology*, 14:291–309.

Fisher, R., T. Vigilante, C. Yates, and J. Russell-Smith, 2003. Patterns of landscape fire and predicted vegetation response in the North Kimberley region of Western Australia, *International Journal of Wildland Fire*, 12(3–4):369–379

Freidl, M.A., and C.E. Brodley, 1997. Decision tree classification of land cover from remotely sensed data, *Remote Sensing of Environment*, 61:399–409.

García, M., and E. Chuvieco, 2004. Assessment of the potential of SAC-C/MMRS imagery for mapping burned areas in Spain, *Remote Sensing of Environment*, 92:414–423.

Gong, P., R.L. Pu, Z.Q. Li, J. Scarborough, N. Clinton, and L.M. Levien, 2006. An integrated approach to wildland fire mapping of California, USA using NOAA/AVHRR data, *Photogrammetric Engineering & Remote Sensing*, 72(2):139–150

Greenbery, C.H., 2003. Vegetation recovery and stand structure following a prescribed stand-replacement burn in sand pine scrub, *Natural Areas Journal*, 23:141–151.

Hall, F.G., Y.E. Shimabukuru, and K.F. Huemmrich, 1995. Remote sensing of forest biophysical structure using mixture decomposition and geometric reflectance models, *Ecological Applications*, 5(4):993–1013.

Hodgson, M.E., J.R. Jensen, J.A. Tullis, K.D. Riordan, and C.M. Archer, 2003. Synergistic use of lidar and color aerial photography for mapping urban parcel imperviousness, *Photogrammetric Engineering & Remote Sensing*, 69(9):973–980.

Holden, Z.A., A.M.S. Smith, P. Morgan, M G. Rollins, and P.E. Gessler, 2005. Evaluation of novel thermally enhanced spectral indices for mapping fire perimeters and comparisons with fire atlas data, *International Journal of Remote Sensing*, 26(21):4801–4808.

Hudak, A.T., and B.H. Brockett, 2004. Mapping fire scars in a southern African savannah using Landsat imagery, *International Journal of Remote Sensing*, 25(16):3231–3243.

Huete, A.R., H.Q. Liu, K. Batchily, and W. van Leeuwen, 1997. A comparison of vegetation indices over a global set of TM images for EOS-MODIS, *Remote Sensing of Environment*, 59:440–451.

Jakubauskus, M.E., K.P. Lulla, and P W. Mausel, 1990. Assessment of vegetation change in a fire-altered forest landscape, *Photogrammetric Engineering & Remote Sensing*, 56(3):371–377.

Joy, S.M., R.M. Reich, and R.T. Reynolds, 2003. A non-parametric, supervised classification of vegetation types on the Kaibab National Forest using decision trees, *International Journal of Remote Sensing*, 24(9):1835–1852.

Key, C., and N.C. Benson, 2003. The Normalized Burn Ratio (NBR): A Landsat TM radiometric measure of burn severity, URL: http://www.nrmsc.usgs.gov/research/ndbr.htm (last date accessed: 03 March 2008).

Koutsias, N., M. Karteris, and E. Chuvieco, 2000. The use of intensity-hue-saturation transformation of Landsat-5 Thematic Mapper data for burned land mapping, *Photogrammetric Engineering & Remote Sensing*, 66(7):829–839.

Larsson, H., 1993. Linear regression for canopy cover estimation in Acacia woodlands using Landsat-TM, -MSS and SPOT HRV XS data, *International Journal of Remote Sensing*, 14(11):2129–2136.

Lawrence, R.L., and A. Wright, 2001. Rule-based classification systems using classification and regression tree (CART) analysis, *Photogrammetric Engineering & Remote Sensing*, 67(10):1137–1142.

Li, D., K. Di, and D. Li, 2000. Land use classification of remote sensing image with GIS data based on spatial data mining techniques, *International Archives of Photogrammetry and Remote Sensing*, 33(B3):238–245.

Maingi, J.K., 2005. Mapping fire scars in a mixed-oak forest in eastern Kentucky, USA, using Landsat ETM+ data, *Geocarto International*, 20(3):51–63.

Maingi, J.K., and W.M. Luhn, 2005. Mapping insect-induced pine mortality in the Daniel Boone National Forest, Kentucky using Landsat TM and ETM+ data, *GIScience & Remote Sensing*, 42(3):224–250.

Marchetti, M., C. Ricotta, and F. Volpe, 1995. A qualitative approach to mapping post-fire regrowth in Mediterranean vegetation with Landsat TM data, *International Journal of Remote Sensing*, 16(13):2487–2494.

McCay, D.H., 2000. Effects of chronic human activities on invasion of longleaf pine forests by sand pine, *Ecosystems*, 3:283–292.

McCay, D.H., 2001. Spatial patterns of sand pine invasion into longleaf pine forests in the Florida Panhandle, *Landscape Ecology*, 16:89–98.

McConnell, K., and E.S. Menges, 2002. Effects of fire and treatments that mimic fire on the Florida endemic scrub buckwheat (*Eriogonum longifolium* Nutt. Var. *gnaphaliafolium* Gand.), *Natural Areas Journal*, 22:194–201.

Miller, J.D., and S.R. Yool, 2002. Mapping forest post-fire canopy consumption in several overstory types using multi-temporal Landsat TM and ETM data, *Remote Sensing of Environment*, 82:481–496.

Myers, R.L., 1990. Scrub and high pine, *Ecosystems of Florida*, (R.L. Myers and J.J. Ewel, editors), University of Central Florida Press, Orlando, Florida.

Pal, M., and P.M. Mather, 2003. An assessment of the effectiveness of decision tree methods for land cover classification, *Remote Sensing of Environment*, 86:554–565.

Patterson, M.W., and S.R.Yool, 1998. Mapping fire-induced vegetation mortality using Landsat Thematic Mapper data: A comparison of linear transformation techniques, *Remote Sensing of Environment*, 65(2):132–142.

Pu, R.L., and P. Gong, 2004. Determination of burnt scars using logistic regression and neural network techniques from a single post-fire Landsat 7 ETM+ image, *Photogrammetric Engineering & Remote Sensing*, 70(7):841–850.

Riaño, D., E. Chuvieco, S. Ustin, R. Zomer, P. Dennison, D. Roberts, and J. Salas, 2002. Assessment of vegetation regeneration after fire through multitemporal analysis of AVIRIS images in the Santa Monica Mountains, *Remote Sensing of Environment*, 79(1):60–71.

Rogan, J., and J. Franklin, 2001. Mapping burn severity in southern California using spectral mixture analysis, *Proceedings of IGARSS 2001 IEEE International Geoscience and Remote Sensing Symposium*, Sydney, Australia, pp. 1681–1683.

Rogan, J., J. Miller, D. Stow, J. Franklin, L. Levien, and C. Fischer, 2003. Land-cover change monitoring with classification trees using Landsat TM and ancillary data, *Photogrammetric Engineering & Remote Sensing*, 69(7):793–804.

Rogan, J., and S.R. Yool, 2001. Mapping fire-induced vegetation depletion in the Peloncillo Mountains, Arizona and New Mexico, *International Journal of Remote Sensing*, 22(16):3101–3121.

Roy, D.R., L. Boschetti, and S.N. Trigg, 2006. Remote sensing of fire severity: Assessing the performance of the normalized burn ratio, *IEEE Geoscience and Remote Sensing Letters*, 3(1):112–116.

Taverna, K., D.L. Urban, and R.I. McDonald, 2005. Modeling landscape vegetation pattern in response to historic land-use: A hypothesis-driven approach for the North Carolina Piedmont, USA, *Landscape Ecology*, 20(6):689–702.

Tucker, C.J., and P.J. Sellers, 1986. Satellite remote sensing of primary production, *International Journal of Remote Sensing*, 7(11):1395–1416.

USGS, 2001. *MLRC Image Preprocessing Procedure*, U.S. Department of Interior.

Vafeidis, A.T., and N.A. Drake, 2005. A two-step method for estimating the extent of burnt areas with the use of coarse-resolution data, *International Journal of Remote Sensing*, 26(11):2441–2459.

Van Lear, D.H., 2000. Recent advances in the silvicultural use of prescribed fire, *Fire and Forest Ecology: Innovative Silviculture and Vegetation Management, Proceedings of the Tall Timbers Fire Ecology Conference, No. 21*, (W.K. Moser and C.F. Moser, editors) Tall Timbers Research Station, Tallahassee, Florida.

Vikhamar, D., and G. Fjone, 2004. Mapping forest parameters using decision trees and multitemporal Landsat ETM+ data, *Proceedings of IGARSS 2004 IEEE International Geoscience and Remote Sensing Symposium*, Anchorage, Alaska, pp. 2365–2368.

White, J.D., K.C. Ryan, C.C. Key, and S.W. Running, 1996, Remote sensing of forest fire severity and vegetation recovery, *International Journal of Wildland Fire*, 6(3):125–136.

(Received 03 October 2006; accepted 30 November 2006; revised 18 January 2007)